0026-895X/03/6401-59–69$7.00
MOLECULAR PHARMACOLOGY
Copyright © 2003 The American Society for Pharmacology and Experimental Therapeutics
Mol Pharmacol 64:59–69, 2003

Vol. 64, No. 1
2415/1074340
Printed in U.S.A.

APETx1, a New Toxin from the Sea Anemone *Anthopleura elegantissima*, Blocks Voltage-Gated Human *Ether-a-go-go*–Related Gene Potassium Channels

SYLVIE DIOCHOT, ERWANN LORET, THOMAS BRUHN, LÁSZLO BÉRESS, and MICHEL LAZDUNSKI

Institut de Pharmacologie Moléculaire et Cellulaire, Centre National de la Recherche Scientifique (CNRS)-Unité Mixte Recherche 6097, Valbonne, France (S.D., M.L.); Institut de Biologie Structurale et Microbiologie, CNRS Unité Propre de Recherche 9027, Marseille, France (E.L.); and the Klinikum der Christian-Albrechts-Universität, Abteilung Toxikologie, Kiel, Germany (T.B., L.B.)

Received January 17, 2003; accepted April 7, 2003

This article is available online at http://molpharm.aspetjournals.org

ABSTRACT

A new peptide, APETx1, which specifically inhibits human *ether-a-go-go*–related gene (HERG) channels, was purified from venom of the sea anemone *Anthopleura elegantissima*. APETx1 is a 42-amino acid peptide cross-linked by three disulfide bridges and shares 54% homology with BDS-I, another sea anemone K^+ channel inhibitor. Although they differ in their specific targets, circular dichroism spectra and molecular modeling indicate that APETx1 and BDS-I have a common molecular scaffold and belong to the same structural family of K^+ channel blocking peptides. APETx1 inhibits HERG currents in a heterologous system with an IC_{50} value of 34 nM by modifying the voltage dependence of the channel gating. Central injections in mice failed to induce any neurotoxic symptoms. APETx1, which has no sequence homologies with scorpion toxins acting on HERG, defines a new structural group of HERG gating modifiers isolated from a sea anemone.

The human *ether-a-go-go*–related gene (*HERG* or erg1) encodes an atypical six transmembrane segment voltage-gated potassium (Kv) channel generating outward currents with inward rectification properties. Erg1 is expressed in mammalian heart, where it contributes to the rapidly activating delayed-rectifier potassium current (IKr) (Sanguinetti et al., 1995; Trudeau et al., 1995). HERG channels are essential in cardiac cells, where they control the duration of the plateau phase of the action potential. Several mutations on the *HERG* gene are responsible for inherited disorders characterized by abnormal, slow repolarization of action potentials associated with long QT intervals on electrocardiograms (Sanguinetti et al., 1996; Spector et al., 1996). This long QT syndrome causes episodic ventricular arrhythmias and ventricular fibrillation, which can result in syncope and sudden death. In the central nervous system, erg channels are thought to be involved in neurite growth, differentiation in normal and tumorous cells, the cell cycle, and spike frequency adaptation (Arcangeli et al., 1995; Chiesa et al., 1997; Bianchi et al., 1998).

The most specific blockers of HERG are the methanesulfonanilide E4031, dofetilide, and ibutilide, which act as "open channel blockers" with a very slow rate of binding (Sanguinetti and Jurkiewicz, 1990; Snyders and Chaudhary, 1996). They behave as class III antiarrhythmic agents but can also lead to arrhythmias. HERG currents are also blocked by other less specific drugs, such as the calcium-channel blockers mibefradil and bepridil (Chouabe et al., 2000), antipsychotic drugs (Suessbrich et al., 1997), histamine receptor antagonists (Taglialatela et al., 1998), antibiotics (Drici et al., 1998), and gastrointestinal drugs such as cisapride. Therapeutic treatments with these drugs can lead, in a small number of persons, to *torsades de pointes* (i.e., potentially fatal arrhythmias) because of their secondary action on HERG channels.

In the last 20 years, animal venoms have provided us with a great number of pharmacological tools that can block, specifically and with a high affinity, a variety of Ca^{2+}-activated, voltage-dependent, and inward-rectifier K^+ channels (Moczydlowski et al., 1988; Grissmer et al., 1994). Bee and scorpion venoms contain toxins blocking Ca^{2+}-activated K^+ channels or G protein-coupled inwardly rectifying K^+ channels (Hugues et al., 1982; Drici et al., 2000). Snake, scorpion, bee, and spider venoms contain toxins that block Kv1, Kv2, and Kv4 channels (Bidard et al., 1989; Schweitz et al., 1989; Awan and Dolly, 1991; Swartz and MacKinnon, 1995; Diochot et al., 1999; Tytgat et al., 1999). In addition, sea-anemone peptides have been found to selectively inhibit Kv1.1,

This work was supported by the Centre National de la Recherche Scientifique, the Ministère de la Recherche et de la Technologie, and the Association Française contre les Myopathies.

ABBREVIATIONS: HERG, human *ether-a-go-go*–related gene; Erg, *ether-a-go-go*–related gene; CD, circular dichroism; TFA, trifluoroacetic acid; HPLC, high-performance liquid chromatography; DTX, dendrotoxin.

Kv1.2, Kv1.3, and Kv3.4 channels (Aneiros et al., 1993; Castaneda et al., 1995; Schweitz et al., 1995; Diochot et al., 1998). Finally, scorpion toxins that target HERG channels have also been described recently (Gurrola et al., 1999; Korolkova et al., 2001). The peptide ErgTx acts as a gating modifier of the HERG channel and seems to bind to the outer vestibule on the S5-P and P-S6 linkers (Pardo-Lopez et al., 2002).

In the present study, we have isolated a new toxin from *Anthopleura elegantissima*, which is the first sea anemone toxin specific for the HERG channel. APETx1 inhibits HERG currents in a voltage-dependent manner by shifting the activation properties of HERG channel. Thus, APETx1, like ErgTx, is probably a gating modifier of the HERG channel. A molecular model was constructed, based on sequence homologies of APETx1 with BDS-I, another K^+ channel inhibitor from sea anemone specific for Kv3.4 channels and inactive on HERG channels, (Driscoll et al., 1989a,b; Diochot et al., 1998). The CD spectra of APETx1 and BDS-I are different but both are typical of β structures and suggest that mutations induce a change in β-turn types. Molecular modeling shows that APETx1 can adopt a fold similar to that of BDS-I despite nonconservative mutations and that the main structural change is located in a loop containing residues 7 to 13. This study suggests that APETx1 and BDS-I belong to the same structural family of K^+ channel-blocking peptides and that similar folding is compatible with different K^+ channel selectivity. The channel selectivity could be caused by different locations of basic residues on the surface of the two toxins.

Materials and Methods

Purification of APETx1 from *A. elegantissima*. The toxin APETx1 was isolated from a crude watery-methanolic extract of the sea anemone *A.elegantissima*. Purification steps included anion exchange chromatography on QAE Sephadex A-25 (45 × 400 mm) eluted with ammonium acetate pH8.3, and two steps of gel filtration on Sephadex G50 in acetic acid 1M. The major peak was lyophilized and diluted (1 mg/ml) with solvent A [0.1% trifluoroacetic acid (TFA) in water] then purified on a Beckman ODS C18 column (10 × 250 mm) using reversed-phase HPLC. A linear gradient from 10 to 40% solvent B (0.1% TFA in acetonitrile) in 30 min was used at a flow rate of 1 ml/min. The UV absorbance of the effluent was monitored at 220 and 280 nm. Further purification steps of the fraction of interest were achieved on a cation exchange column TSK-SP 5PW (7.5 × 75 mm) (Toyosoda, Tokyo, Japan) with a linear gradient from 0 to 100% solvent D (1 M ammonium acetate) in 50 min. The major peak included the HERG channel-blocking peptide and was finally purified using the same reversed-phase HPLC conditions described above.

Peptide Sequencing and Mass Determination. The APETx1 peptide was reduced with 2-mercaptoethanol and pyridylethylated with 4-vinylpyridine then sequenced using the Edman degradation method on a microsequencer (model 477A; Applied Biosystems, Foster City, CA). Molecular mass was determined by electrospray ionization mass spectrometry. Samples were dissolved in 20% acetonitrile/water, 0.1% HCOOH (5–10 pmol/μl). Ion spray mass spectra were recorded on a simple-quadrupole mass spectrometer (API I; PerkinElmerSciex Instruments, Boston, MA) equipped with an ionspray (nebulizer-assisted electrospray) source (MDS Sciex, Toronto, Canada). The system was connected to an Apple Macintosh equipped with Tune v2.4.1 and MacSpec v3.3 (PerkinElmerSciex) software for instrument control, data acquisition and data processing. Solutions were continuously infused with a medical infusion pump (model 11; Harvard Apparatus, South Natick, MA) at a flow rate of 5 μl/min. Polypropylene glycol was used to calibrate the quadrupole. Ion spray mass spectra were acquired at unit resolution by scanning from m/z 600 to 1600 with a step size of 0.1 Da and a dwell time of 2 ms. Five spectra were summed. The potential of the spray needle was held at +4.5 kV. Spectra were recorded at an orifice voltage of +90V. Mac BIO Spec software was used for calculation of the molecular masses of the samples. Theoretical molecular masses were calculated from sequence data using GPMAW protein analysis software.

Mouse Intracisternal Injections. Anesthetized 5-week-old Balb/C mice were injected intracisternally with 1 to 5 μl of APETx1 solutions. APETx1 was dissolved in a NaCl solution (0.9%) supplemented with 0.1% bovine serum albumin (BSA). Symptoms were observed and noted for the first hour after injections and at regular intervals for the subsequent 24 h.

Cell Cultures and Transfections. COS-7 cells were prepared as described previously (Chouabe et al., 1998). A total of 20,000 cells was plated on 35-mm Petri dishes and transfected using the DEAE-dextran/chloroquine method. pSI-HERG plasmid (0.05 μg) was used in each dish. For toxin specificity experiments, 0.01 μg of pCI-Kv1.1, pCI-Kv1.2, pCI-Kv1.3, pCI-Kv1.4, pCI-Kv1.5, pCI-Kv1.6, pCI-Kv2.1, and pRc/CMV Kv3.4; 0.05 μg of pCI-Kv4.2; 0.5 μg of pCI-IRES-CD8-KCNE2, pCI-KCNQ1, pCI-KCNQ2, pCI-KCNQ3; and 1 μg of pCI-EAG1 and pCI-ELK1 were used per dish. A CD8-expressing plasmid (one fifth of the required K^+ channel-expressing plasmid) was added in all transfection experiments to visualize transfected cells using anti-CD8 antibody-coated beads. NG108-15 cells (mouse neuroblastoma X rat glioma cells) were cultured and differentiated as described previously (Robbins et al., 1992).

Electrophysiological Measurements. Currents were recorded in COS-7 cells within 1 to 2 days after transfection, at room temperature (22°C) in the whole-cell configuration of the patch-clamp technique. The standard external solution (also used for NG108-15 cells) contained 150 mM NaCl, 5 mM KCl, 1 mM $CaCl_2$, 3 mM $MgCl_2$, 5 mM glucose, and 10 mM HEPES-NaOH at pH 7.4. The intracellular pipette filling solution contained 150 mM KCl, 3 mM $MgCl_2$, 5 mM EGTA, and 10 mM HEPES-KOH at pH 7.4. BSA (0.1%) was added in toxin-containing solutions to prevent their adsorption to plastic tubes.

Cells were perfused continuously with the external solution. Patch pipettes with a resistance of 2–5 MΩ were used and connected electrically to the head stage of a RK300 patch-clamp amplifier (Biologic, Grenoble, France). Junction potentials were zeroed with the pipette in the standard extracellular solution. Membrane capacitance and series resistance were not compensated. Voltage commands and simultaneous signal recording were performed with pClamp software (Axon Instruments, Union City, CA). Solutions were applied using a perfusion system (200-μm i.d. capillary tubing; flow rate, 0.3 ml/min) placed in the proximity of the cell (<1 mm) in a 2-ml bath chamber, which allowed the extracellular environment of the cell to be changed within a few seconds.

M-like currents from differentiated NG108-15 cells were recorded using amphotericin B perforated-patch electrodes as described by Selyanko et al. (2002).

Pulse Protocols and Analysis. HERG currents were evoked every 10 s by 3-s depolarizing voltage steps ranging from −60 to +50 mV in 10-mV increments and then by a repolarizing step to −40 mV for 1.5 s. Dose-response curves were fitted using the Hill equation $I = I_{max} + (I_{min} - I_{max})\,[C^{n_H}/(C^{n_H} + IC_{50}{}^{n_H})]$, where I is the amplitude of relative current, I_{max} is the maximum current amplitude, I_{min} is the minimum current amplitude, C is the concentration of the toxin, IC_{50} is the concentration of toxin that induces half-inhibition of the current represented by $I_{max} - I_{min}$, and n_H is the Hill coefficient. Current-voltage relations were measured on depolarized steady-state currents at the end of 3-s pulses. Conductances were measured on the peak of the HERG tail current upon repolarization to −40 mV. The activation curve was fitted with the Boltzmann equation: $G = G_{max}/[1 + \exp(V_{0.5} - V)/k]$, where $V_{0.5}$ is the half-activation potential

and k is the curve slope. G was normalized to the peak membrane conductance at +50 mV (G_{max}). Steady-state inactivation was assessed after a long pulse (300 ms) to +50 mV by brief steps (25 ms) from −120 mV to +80 mV in 10-mV increments every 7 s. After allowing inactivation to relax to steady state at various voltages, the membrane potential was stepped to +50 mV to assess the relative number of channels available for activation. The tail current (measured at the peak of the second step to +50 mV) was plotted as a function of the previous voltage step. Deactivation at negative voltages was not corrected. Normalized data points were fitted to a Boltzmann distribution. For toxin specificity studies, Kv1.n, Kv2.1, Kv3.4, Kv4.2, EAG1, ELK1, and KCNQ currents were evoked by depolarizing voltage steps between −10 mV and +30 mV from a −80-mV holding potential. Results are expressed as mean ± S.E. The statistical significance of differences between sets of data were estimated by single-sided Student's t test.

M-like currents (I_K(M,ng) have been described in various cells, including NG108-15 neuroblastoma. They share similar electrophysiological and pharmacological properties with the M-current described in sympathetic neurons (Brown and Adams, 1980). There are data to support the concept that deactivation currents in NG108-15 cells consisted of two components, including KCNQ2/Q3 (the M-like current) and ERG1/ERG2 (ERG current) (Meves et al., 1999; Selyanko et al., 2002). Deactivation currents were recorded after hyperpolarizing the cells to −50 mV from a holding potential of −20 mV. M-like currents showed characteristic deactivation tails. Inhibition of the current was measured from the amplitude at the peak of the deactivation tail current.

Drugs. All drugs were stored as stock solutions at −20°C: 1 mM BDS-I (purified in our laboratory from *Anemonia sulcata* extracts) in distilled water, 10 mM dofetilide (Tikosyn; Pfizer Inc., New York, NY) in DMSO, 1 mM E4031 (Eisai Ltd, Ibaraki, Japan) in distilled water. BSA and amphotericin B were from Sigma (St. Louis, MO).

Circular Dichroism. CD spectra were measured in the range from 260 to 178 nm on a Jobin-Yvon (Long-Jumeau, France) UV CD spectrophotometer (MARK VI). The instrument was calibrated with (+)-10-camphorsulfonic acid, and a ratio of 2:1 was found between the positive CD band at 290.5 nm and the negative band at 192.5 nm. The measurements were carried out at 20°C using 0.005-cm pathlength cells. Spectra were recorded in 20 mM phosphate buffer, pH 7, at a protein concentration of 1 mg/ml, and the buffer background was subtracted. Data were collected at an interval of 0.5 nm with a scan rate of 3 nm/min. CD spectra was reported as $\Delta\epsilon$ per amide.

Molecular Modeling. The model was built using Insight II software from MSI Technologies, Inc. (San Diego, CA), running on an SGI O_2 workstation (SGI, Mountain View, CA). The model was optimized with the consistent valence force field (CVFF) in terms of internal energies, using the van der Waals energy to monitor each step of the model. Minimization was performed with steepest descent and conjugate gradient algorithms. Dynamic was performed at 300 K for 1.1 ps using 1000 steps.

Results

Purification of a HERG Channel Inhibitor from *A. elegantissima*. The aim of our study was to purify new high-affinity natural ligands for HERG potassium channels. To achieve this goal, we fractionated a pool of peptide (14 mg), extracted from the sea anemone *A. elegantissima*, after anion exchange chromatography and gel filtration. We followed the activity of each fraction by its ability to inhibit HERG currents generated after transient expression in COS-7 cells. One fraction that produced an 80% inhibition of HERG currents was then purified using reversed-phase and cation exchange chromatography (Fig. 1). The purified peptide (900 μg) was called APETx1.

Biochemical Properties. APETx1 is a basic (pI = 9.28) 42-amino acid peptide cross-linked by three disulfide bridges. Its full sequence was established by N-terminal Edman degradation of the reduced alkylated toxin. The calculated molecular mass (4,552.21 Da) was in accordance with the measured molecular mass (4,551.99 Da) suggesting a free carboxylic acid at the C-terminal extremity. Its molecular absorbance at 280 nm is ϵ_{280} = 12,810. APETx1 displays no substantial sequence homologies with other sea anemone toxins identified to date (Fig. 2). The highest homologies (54%) are shared with the BDS-I and BDS-II from *A. sulcata*, which inhibit the Kv3.4 potassium current (Diochot et al., 1998). Sequence homologies with Na^+ channel activators (AP-A, AP-B, AP-C, APE-1.n, APE-2) from *Anthopleura* species are only of 35 to 43%. APETx1 shows only 20% homology with ErgTx, a toxin isolated from the scorpion *Centruroides noxius* venom, which also blocks HERG channels (Gurrola et al., 1999).

Circular Dichroism Spectra. Figure 3 shows the comparative CD spectra of APETx1 and BDS-I. The spectra are different, although they remain typical of β structures [for a review see (Johnson, 1985)]. There is no α-helix in the BDS-I three-dimensional structure (Driscoll et al., 1989a,b), and no evidence for α-helix was detected in the APETx1 CD spectrum. The CD spectrum of an α-helix is characterized by three CD bands: a positive and a negative contribution at 190 and 207 nm, respectively, caused by π-π^* transitions, and a negative contribution at 222 nm caused by n-π^* transitions (Johnson, 1985). In the two CD spectra, there are no n-π^* transitions at 222 nm. The APETx1 CD spectrum has a positive contribution at 190 nm and a negative contribution at 204 nm. The intensity of the positive contribution at 190 nm is lower than the negative contribution, which confirms that these contributions are not caused by the α-helix. CD spectra of β-turns have a low intensity (Johnson, 1985). The π-π^* and n-π^* transitions for β-sheet are usually a positive band at 200 nm and a negative band at 215 nm; a change in β-sheet can not explain the differences observed between the two spectra. On the other hand, the π-π^* transition of β-turns can be very different depending on turn type (Johnson, 1985). The differences observed between the two CD spectra can be explained only by a change in β-turn. APETx1 and BDS-I have CD spectra dominated by contributions of β-turns but the conformation of at least one β-turn is different between APETx1 and BDS-I.

Molecular Modeling of APETx1. A model of APETx1 was built from the two-dimensional NMR structure of BDS-I (Driscoll et al., 1989a,b), (Protein Data Bank codes 1BDS and 2BDS) available in the Brookhaven data bank. However, only atomic coordinates of α carbons of BDS-I from residues 1 to 7 and 15 to 43 were used as templates for APETx1. Residues 15 to 43 from BDS-I have a high sequence homology with residues 13 to 41 from APETx1. The atomic coordinates of lateral chains of APETx1 from residues 1 to 7 and 13 to 41 were generated from their corresponding α carbons and located to have no overlaps with other lateral chains. Their orientations were similar to those of the lateral chains in BDS-I. It was not possible to use the full backbone of BDS-I as a template for APETx1. Two gaps are necessary, between residues 7 and 13, to have the six cysteines aligned and the best sequence homology between the two proteins. Moreover, circular dichroism data suggest that at least one loop constituted by a

β-turn has a different conformation in the two proteins. Furthermore, there is no sequence homology with BDS-I between residues 7 and 13. Random loops were generated to connect residue 7 to residue 13 of APETx1. A loop was selected that had no overlap with atoms already in place and had hydrophobic lateral chains heading to the core of APETx1 and hydrophilic lateral chains facing the solvent. Finally, Asp 42 was added to complete the model of APETx1. An initial minimization step with free cysteines was carried out; no change in the orientation of the lateral chains of cysteines was observed. This result indicates that the mutations do not induce structural changes susceptible to modify the regular disulfide bridge pattern of the sea anemone peptides (Driscoll et al., 1989a,b). Therefore, the three disulfide bridges were created similarly to BDS-I. The BDS-I three-dimensional structure used to build the APETx1 model has a van der Waals energy of 192 kcal/mol, which was used as a target energy level for the APETx1 model. Energy minimization and dynamics made it possible to dramatically reduce van der Waals energy to 220 kcal/mol to obtain the final APETx1 model (Fig. 4). The molecular modeling of APETx1 shows that the mutations do not induce a different folding compared with BDS-I. Even the substitution of Pro-36 in *cis* configuration in BDS-I to Leu-34 in APETx1 does not alter the conformation of the loop where these residues are located (Fig. 4). The main structural change is located between residues 7 and 12, as would be expected, but this change had no apparent influence on the disulfide bridge between Cys-4 and Cys-37. However, the mutations do induce a dramatic change in the location of charged residues (mainly basic) compared with BDS-I. Charged residues in BDS-I, such as Arg-12, Asp-14, Arg-19, and Lys-34, are substituted in APETx1, respectively (if we take into account the gap of two residues in the N-terminal loop), to Ile-10, Ile-12, Thr-17, and Tyr-32 (see also Fig. 2). Interestingly, there is a compensation with the substitutions of Tyr-26 and Gly-20 in BDS-I to Arg-24 and Lys-18 in APETx1. The model shows also that the lateral chain of Trp-35, which is accessible to the solvent in BDS-I, is substituted by the lateral chain of Lys-18 in APETx1. Trp-35 in BDS-I is replaced by Phe-33 in APETx1, but the lateral

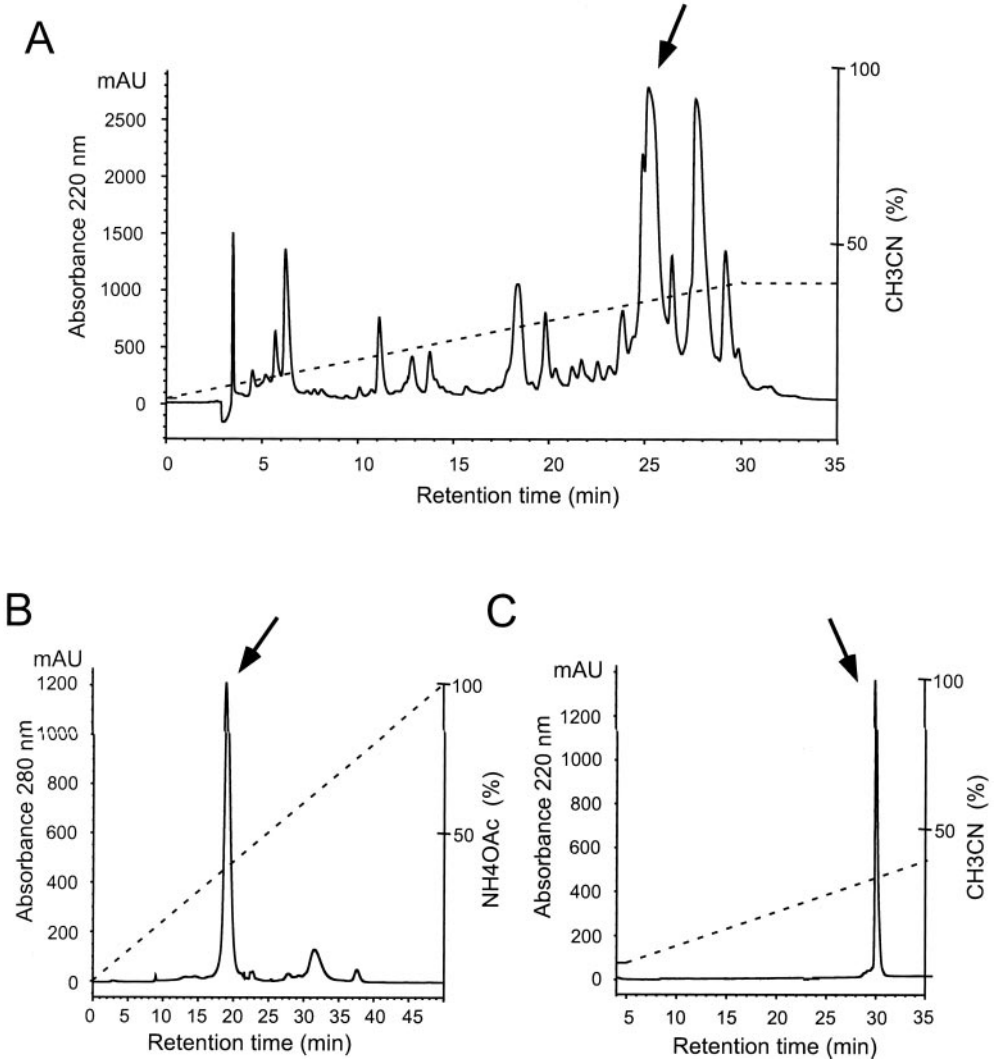

Fig. 1. HPLC purification of APETx1. A, the sea-anemone polypeptide active on HERG was loaded on a reversed-phase C18 column with a linear gradient (dashed line) of acetonitrile/TFA. Only one of the fractions corresponding to the arrow was active on HERG current. B, cation exchange chromatography of the active peak eluted with a linear gradient of ammonium acetate (dashed line). Arrow, fraction containing HERG blocking peptide. C, final step of purification of the active peak on reversed phase C18 column eluted with the same solvent as in A. The pure APETx1 peptide is indicated (arrow).

chain of Phe 33 is not accessible to the solvent in APETx1. Finally, the model shows that Lys-8 in BDS-I that seems to be conserved with Lys-6 in APETx1 does not have the same location because of the structural change of the N-terminal loop (Fig. 4).

Effects of APETx1 on HERG Channels. HERG currents were recorded on COS-transfected cells. Outward currents were recorded after depolarizations from a holding potential of −80 mV and peak currents (I_{peak}) measured at the end of 3-s pulses. Upon repolarization to −40 mV, an outward tail current (I_{tail}) was recorded. The amplitude of I_{tail} increased with depolarizing steps from −40 to +30 mV, and then current traces were superimposed on further depolarizing steps to +50 mV. During perfusion of APETx1 (10 to 100 nM), not only I_{peak} (recorded at 0 mV) but also I_{tail} were inhibited (Fig. 5A). The blockade was rapid (steady-state reached in 1 min) and totally reversible upon washout (Fig. 5B). The dose-response curve showed the HERG inhibition measured on peak I_{tail} currents. The IC_{50} value was 34 nM (n_H = 1.4) and the inhibition is maximal at 300 nM leaving part (20%) of the current unblocked even at concentrations up to 1 μM (Fig. 5, C and D). Antiarrhythmic methanesulfonanilide drugs such as dofetilide (300 nM) or E4031 (1 μM) blocked this APETx1-resistant current (Fig. 5D). The dose-response curves for HERG inhibition by dofetilide and E4031 indicated that IC_{50} values were 48 and 28 nM, respectively (data not shown).

In Fig. 6A, the voltage-dependence of activation of the HERG channels was presented with the I_{tail} normalized. The mean half-maximal activation ($V_{0.5}$) was +1 ± 5 mV in control conditions. In the presence of APETx1 (100 nM), a 19-mV shift of the activation curve toward positive potentials was observed ($V_{0.5}$ = +20 ± 8 mV, n = 5, significantly different from the control value, P = 0.0043), so that the amplitude of I_{tail} was decreased in a voltage-dependent manner. The effect of APETx1 was voltage-dependent: at 0 mV, 100 nM APETx1 inhibited 68% of the current, whereas only 25% was inhibited at +30 mV. The voltage-dependence of inhibition by APETx1 was also clearly demonstrated in Fig. 6A, inset. The inset illustrates current-voltage relations before and after application of 100 nM APETx1 where greater inhibition occurred at 0 mV compared with +30 mV. Averaged, normalized inactivation relation showed a 25-mV negative shift of the curve, $V_{0.5}$ values are −22 ± 6 mV in control (n = 4) and −47 ± 7 mV (n = 4, significantly different from the control value, P = 0.0014) with 50 nM APETx1 (Fig. 6B).

Because drugs such as class III antiarrhythmic agents preferentially block open HERG channels (Snyders and Chaudhary, 1996; Spector et al., 1996), we compared the use dependence of the current inhibition by the toxin under repetitive pulses at 0 mV from a holding potential of −80 mV using pulse intervals of either 1 or 10 s. The steady-state of inhibition by APETx1 (50 nM) was obtained within 101 ± 19 s (n = 6) and 64 ± 13 s (n = 11, values are significantly different, P = 0.0003) during depolarization pulses every 1 and 10 s, respectively (Fig. 6C). The time course of current inhibition was fitted by a single exponential and the time constants (τ) were 45 ± 2 s (n = 6) and 26 ± 8 s (n = 11), respectively, in each condition. Thus, HERG current inhibition is more rapid when the frequency of depolarization is slow and the amplitude of the blockade was not dependent on the activation frequency. When APETx1 (50 nM) was perfused for 1 min on cells held at −80 mV, the current recorded from the first depolarizing pulse was inhibited by 60 ± 8% (n = 6; Fig. 6D). No additional inhibition was recorded during further depolarizing pulses. We concluded that APETx1 alters the voltage-dependence of HERG gating in the absence of pulsing.

Effects of APETx1 on Other Cloned K^+ Channels. APETx1 at 100 nM, a concentration that blocks HERG currents by 75%, was tested on various other cloned Kv channels expressed in COS-7 cells. Except for the Kv1.4 channel, which was only slightly inhibited (27 ± 10% n = 3), none of

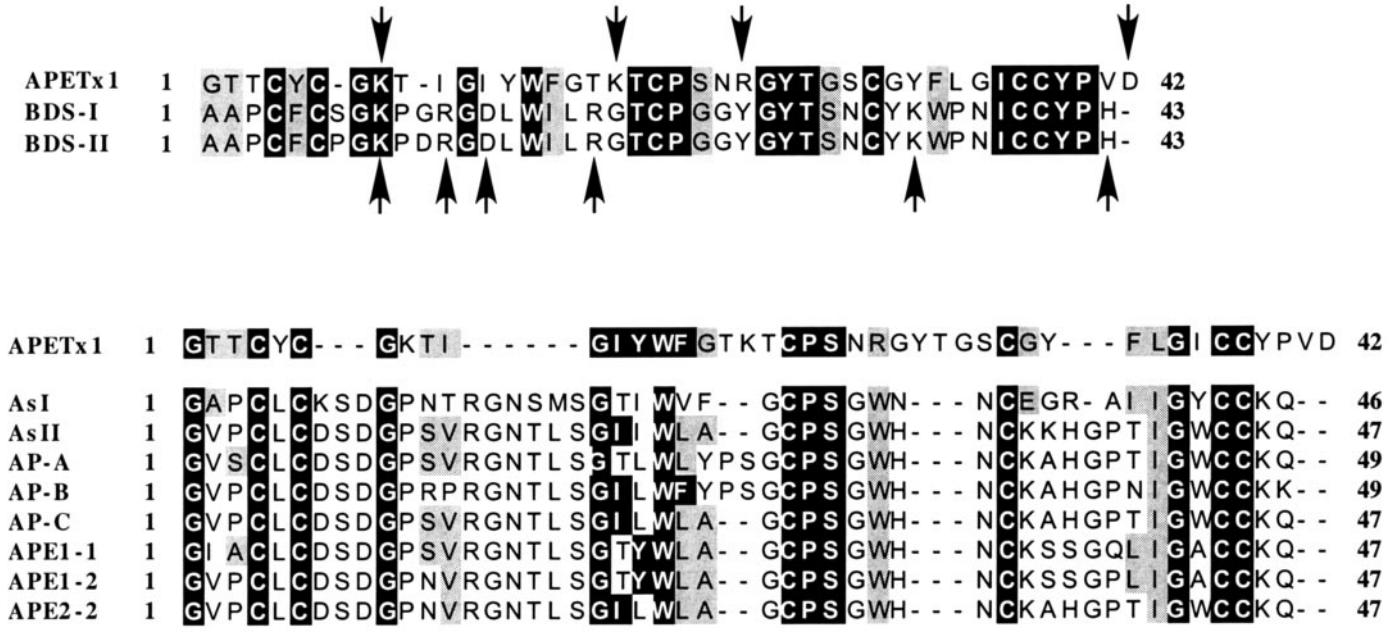

Fig. 2. Sequence alignments of APETx1, with Na^+ and K^+ channel modulators from sea anemones. Black boxes indicate sequence identities and gray boxes sequence similarities with BDS-I, BDS-II, AsII from *A. sulcata*, AP-A and AP-B from *Anthopleura xanthogrammica*, and AP-C, APE1–1, APE1–2, and APE2–2 from *A. elegantissima* (Bruhn et al., 2001). Charged residues are indicated by arrows in BDS-I, BDS-II, and in APETx1.

the other channels tested (Kv1.(1–6), KCNQ1–3, KCNQ1+IsK1, Kv2.1, Kv3.4, and Kv4.2) were significantly inhibited by APETx1 (Fig. 7). Even higher concentrations of APETx1 (1 μM) did not strongly reduce the Kv1.4 current (35 ± 8% n = 5). In addition, other members of the eag family, such as EAG1 (n = 5) and ELK1 (n = 6) were insensitive to 100 nM APETx1.

Effect of APETx1 on the M-Like Current ($I_{K(M,ng)}$) of NG108-15 Cells. The M-like currents are analogous to the M current described in sympathetic neurons, which exert an inhibitory control over neuronal excitability (Brown and Adams, 1980). M-like currents were identified in a variety of neural and non-neuronal cells. We recorded such currents on differentiated NG108-15 cells using the perforated-patch method. Typical outward deactivating tail currents were observed during the hyperpolarizing steps from a holding potential of −20 mV. This current has two components mediated by two types of K^+ channels. One is a fast component probably carried by KCNQ2/Q3 (M-like current); the other is a slow component mediated by ERG1/ERG2 (ERG current) (Meves et al., 1999; Selyanko et al., 2002). As illustrated in Fig. 8, APETx1 at a concentration of 30 nM inhibited 41 ± 12% and 29 ± 7% (n = 4) of the peak and the sustained (measured at the end of a −50 mV hyperpolarizing pulse) deactivating tail current, respectively. A higher concentration (100 nM) inhibited the peak of the deactivation (by 55 ± 10%, n = 4), but was without effect on the residual fast component of the current (Fig. 8*C*). The standing (−20 mV) outward current was also significantly reduced. Effects were rapid (steady-state inhibition occurred after 40 s) and reversible. The blockade was maximal at 100 nM; APETx1 (300 nM) failed to induce further inhibition. These results suggest that APETx1 inhibited the slow component mediated by ERG channels, leaving the fast component carried by KCNQ2/Q3 channels unblocked.

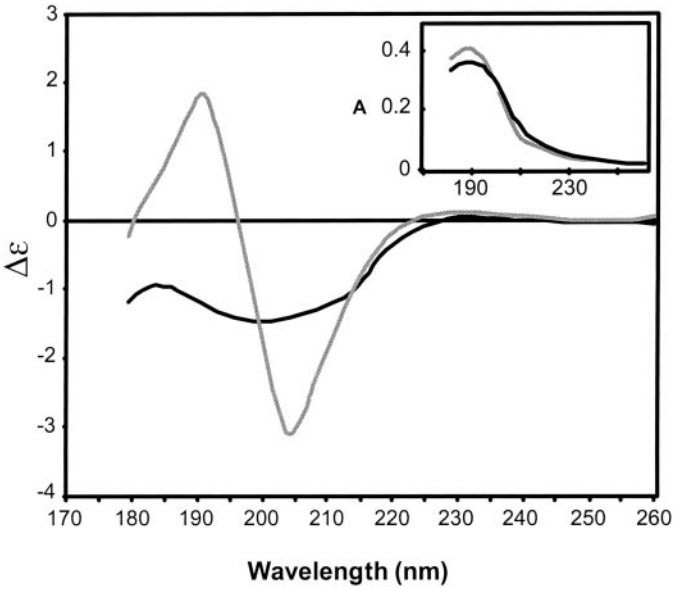

Fig. 3. CD spectra of APETx1 and BDS-I. CD spectra were measured from 260 to 178 nm and data are expressed in Δε per amide. Absorbance spectra for the two proteins, APETx1 (gray) and BDS-I (black), are shown in the left corner and indicate that the concentration, 1 mg/ml, was similar for the two proteins during the measurement. The two CD spectra are different but they remain typical of contribution as a result of β-turn (Johnson, 1985). Conformational differences in a β-turn might explain the difference in the two CD spectra.

In vivo central injections of APETx1. Several toxins that specifically inhibit Kv1.1, Kv1.2 and Kv1.6 channels, such as mast-cell degranulating peptide or dendrotoxin (DTX), induce severe neurotoxicity after central injection into the mammalian central nervous system (Schweitz, 1984; Mourre et al., 1997). Because erg1 transcripts are widely distributed in mammalian brain, we wanted to observe the consequences of central injection of APETx1 in mice to investigate the role of erg channels in the central nervous system. Intracisternal injections of 100 pmol (0.45 μg, n = 2), 1 nmol, and 2 nmol (4.5 and 9 μg, respectively, n = 3) of APETx1 did not induce any neurotoxic symptoms in mice even after 24 h.

Discussion

In the 1970s, a large number of highly neurotoxic and cardiotoxic peptides were first isolated from sea anemone nematocysts. These toxins prolonged the repolarization phase of the action potential of axons, cardiac cells, and neuroblastoma cells (Romey et al., 1976) and induced positive inotropic effects on mammalian heart strips (Renaud et al., 1986). Their target was found to be voltage-sensitive Na^+ channels (Na_v) (Frelin et al., 1984). Major structural deter-

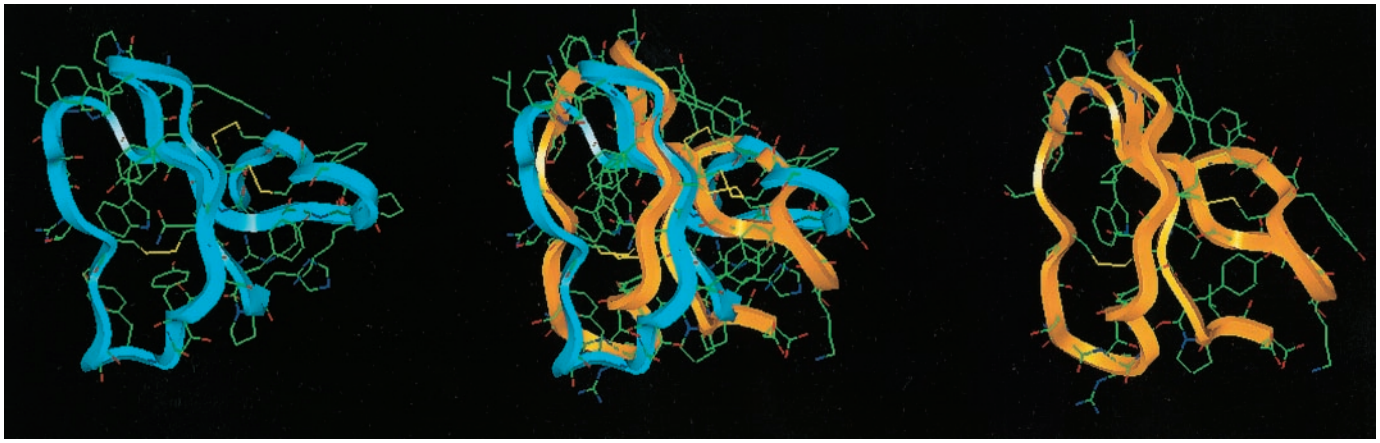

Fig. 4. Molecular modeling of APETx1 based on the structure of BDS-I. The atomic coordinates of αcarbons of BDS-I (blue ribbon) (Driscoll et al., 1989a,b) were used as template to build the APETx1 (orange ribbon) model. Energy minimization and dynamic were used to refine the APETx1 model. A similar folding is observed for the two proteins with a local variation in the N-terminal loop. This local variation is caused by a conformational change of a β-turn, as suspected from the CD spectra analysis.

minants of sea anemone toxin binding to Na_v channels have been identified. These toxins bind with high affinities to the S3-S4 extracellular loop of Na_v channels, modifying their inactivation kinetics (Benzinger et al., 1998; Bruhn et al., 2001). Na_v toxins from sea anemones have been useful tools to understand Na^+ channel structure and function (Norton, 1991).

More recently, other less toxic peptides from sea anemones have been discovered that affect Ca^{2+}-activated K^+ channels and voltage-dependent K^+ (Kv) channels (Rauer et al., 1999). Sea anemones have developed several toxins that selectively block Kv1 or Kv3 channels. ShK from *Stichodactyla helianthus*, BgK from *Bunodosoma granulifera*, AsKS from *A. sulcata*, and HmK from *Heteractis magnifica* are homologous toxins that block with picomolar to nanomolar affinities the Kv1.1, Kv1.2, and Kv1.3 channels (Aneiros et al., 1993; Castaneda et al., 1995; Schweitz et al., 1995; Cotton et al., 1997; Gendeh et al., 1997). They belong to the first structural group of short peptides with 35 to 37 amino acids (Fig. 9). ShK and BgK three-dimensional structures consist of two short α-helices and one helical turn stabilized by the three disulfide bridges, one of them linking the two helices (Dauplais et al., 1997). The second group includes kalicludines, 57- to 60-amino acid peptides isolated from *A. sulcata* that compete with ^{125}I-DTX_I for binding to Kv1.2 channels. They share sequence homologies with basic pancreatic trypsin inhibitor and DTX_I. Their secondary structures consist of two-stranded β-sheet and two α-helices (Lancelin et al., 1994; Schweitz et al., 1995) (Fig. 9). The third group is represented by the toxins BDS-I and BDS-II, which selectively inhibit Kv3.4 channels (Diochot et al., 1998). They are 43-amino acid peptides cross-linked by three disulfide bridges, and their three-dimensional structure is based on a triple-stranded antiparallel β-sheet without α-helix (Driscoll et al., 1989a,b) (Fig. 9).

In this work, we have isolated APETx1, a new toxin from *A. elegantissima* that inhibits the HERG potassium channel, which underlies the I_{Kr} cardiac current. This is the first sea anemone toxin to bind to a member of the EAG family of voltage-dependent K^+ channels. Two scorpion toxins, ErgTx from *C. noxius* and BeKm-1 from *Buthus epeus,* have been described recently as potent inhibitors of HERG channels (Gurrola et al., 1999; Korolkova et al., 2001). APETx1, ErgTx, and BeKm-1 share no sequence homologies, and the differences in the positions of their cysteine residues suggest that they belong to three different structural groups of toxins.

The primary structure of APETx1 shows that it does not belong to the group of voltage-dependent Na^+ channel toxins (Fig. 2). However, APETx1 shares 54% sequence homology with the BDS toxins, and circular dichroic spectra show an important contribution of β-turns. Molecular modeling of APETx1 revealed similar folding and probably a common disulfide bridge pattern to BDS-I and BDS-II. The APETx1 model also suggests a complete reorganization of the location of the basic residues on the surface of the protein compared with BDS-I (Fig. 2, 4, and 9). Basic residues are suspected to be the main functional residues in scorpion and sea anemone toxins (Loret et al., 1994), and the different location of the basic residues may account for the respective selectivity of APETx1 and BDS-I on K^+ channel subtypes.

The action of APETx1 on HERG channels is voltage-dependent and characterized by a shift of the activation curve

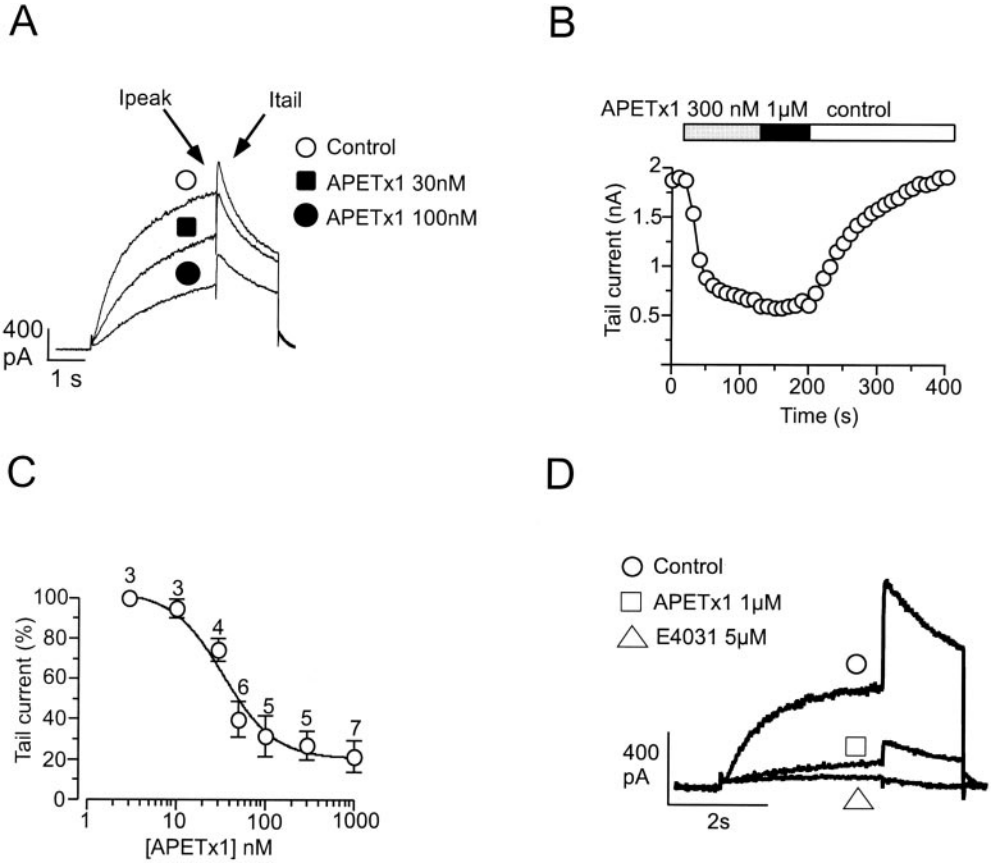

Fig. 5. Effect of APETx1 on HERG currents. HERG currents were recorded in transfected COS-7 cells in the whole-cell configuration of the patch-clamp technique. Holding potential, −80 mV. A, effects of 30 nM and 100 nM APETx1 (■ and ●) on HERG currents (○), recorded upon depolarization at 0 mV and repolarization at −40 mV. B, kinetics of HERG currents during inhibition by 300 nM and 1 μM APETx1 and reversibility. Currents were evoked at 0 mV and quantitatively analyzed upon repolarization at −40 mV. C, concentration-response relationship for APETx1 block of HERG currents evoked as in A. The dose-response curve was fitted by the Hill equation. The IC_{50} value is 34 nM and the Hill coefficient (n_H) is 1.4. Each point is the mean ± S.E.M. of data from three to seven cells. D, effect of 1 μM APETx1 (□) and 5 μM E4031 (△) on HERG currents (○), recorded upon depolarization at 0 mV and repolarization at −40 mV.

toward positive potentials, resulting in a less important blockade when cell membranes are depolarized (i.e., when channels are opened). APETx1 also induces negative shifts of the inactivation curve. The inhibition occurs more rapidly when the cell membrane is hyperpolarized, suggesting a preferential affinity of the toxin to the closed state of the channel. This mode of action is rather different from that of ErgTx, which does not shift the activation curve of the HERG current (Gurrola et al., 1999). Nevertheless, APETx1 and ErgTx are both able to bind to the closed state of HERG channels with nearly the same affinity. Thus, APETx1 is probably not a channel pore blocker but is rather a gating modifier, because the maximal inhibition of HERG currents by saturating concentrations of APETx1 is only 80%. APETx1 may interact with residues located on the outer vestibule of the channel pore, as already suggested for ErgTx (Pardo-Lopez et al., 2002).

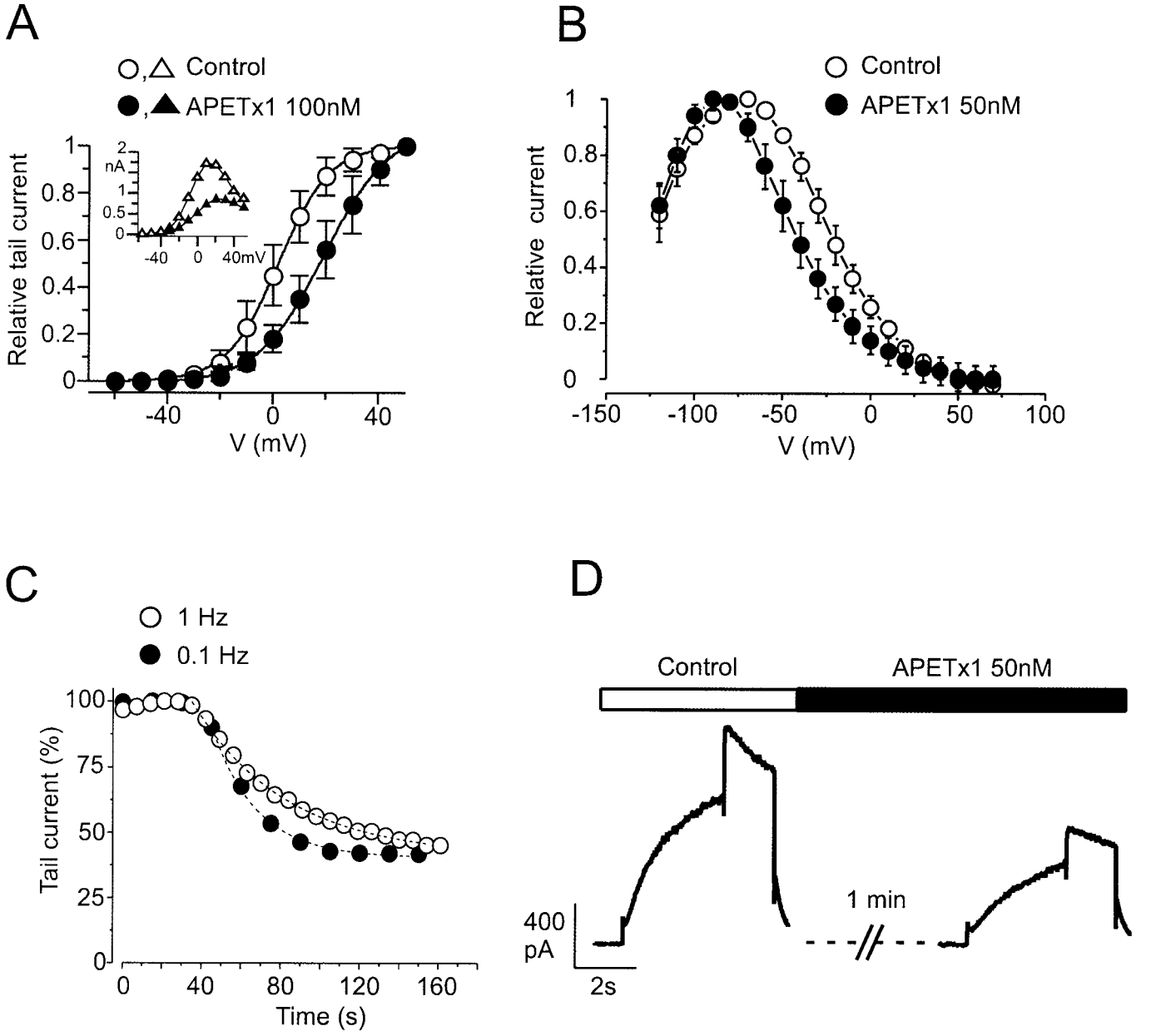

Fig. 6. Voltage-dependent effects of APETx1 on HERG currents. A, normalized and averaged conductance-voltage relationship for HERG currents under control conditions (○) and after application of 100 nM APETx1 (●). Conductances were measured on the tail current upon repolarization to −40 mV. The curve was fitted as described in experimental procedures. Averaged half-point activation values for $V_{0.5}$ and the corresponding slope factor k were: $V_{0.5}$ = 1 ± 5 mV, k = 9 ± 1 (control) and $V_{0.5}$ = 20 ± 8 mV, k = 12 ± 2 (APETx1). Values are means of five experiments in each condition. Inset, current-voltage relations for HERG current in control conditions (△) and after application of 100 nM APETx1 (▲). Currents were measured on peak currents at the end of 3-s depolarizing pulses. B, steady-state inactivation curves in control conditions (○) and after application of 50 nM APETx1 (●). The plotted points show normalized peak current released from inactivation at +50 mV against test potential. The mean value of HERG half-point inactivation $V_{0.5}$ and the corresponding slope factor k were: $V_{0.5}$ = −22.5 ± 6 mV, k = 17.8 ± 0.4 (control) and $V_{0.5}$ = −47 ± 7 mV, k = 20 ± 1.2 (APETx1) (n = 5 cells, $P < 0.005$). C, the time course of current inhibition by APETx1 (50 nM) under repetitive depolarizations was measured upon repolarization at −40 mV. Cells were depolarized to 0 mV from a holding potential of −80 mV using pulse intervals of either 1 (○) or 10 s (●). The fit by a single exponential (dashed lines) of the current decay gives time constants (τ) of 47.5s (○) and 25.8s (●) respectively. D, effect of APETx1 (50 nM) on closed HERG channels. The toxin was perfused (black bar) for 1 min and cell membranes were held at −80 mV. The current traces, recorded during a depolarization at 0 mV and a repolarization to −40 mV, are shown in control (stack bar) and under perfusion with APETx1.

The mode of action of APETx1 differs from those of class III anti-arrhythmics that also target HERG channels. These drugs act like open channel blockers. Dofetilide blocked HERG currents with an affinity (IC_{50}) of 12 nM in human embryonic kidney 293 cells (Snyders and Chaudhary, 1996) and 48 nM in COS-7 cells (present study), which is near the affinity of APETx1 observed for HERG channels (IC_{50} of 34 nM). However, the two classes of drugs act by different mechanisms because dofetilide, which is an open channel blocker, is unable to block HERG currents when cell membranes are polarized (i.e., when channels are closed) (Finlayson et al., 2001). Moreover, in contrast to APETx1, dofetilide inhibition is slow (Snyders and Chaudhary, 1996; Finlayson et al., 2001). Peptides isolated from animal venoms are rather bulky molecules compared with class III antiarrhythmics and are not able to cross cell membranes. In particular, it is not surprising that their binding site is located on external parts of the channel more accessible during closure, because the access to an intracellular binding site would be dependent on channel opening.

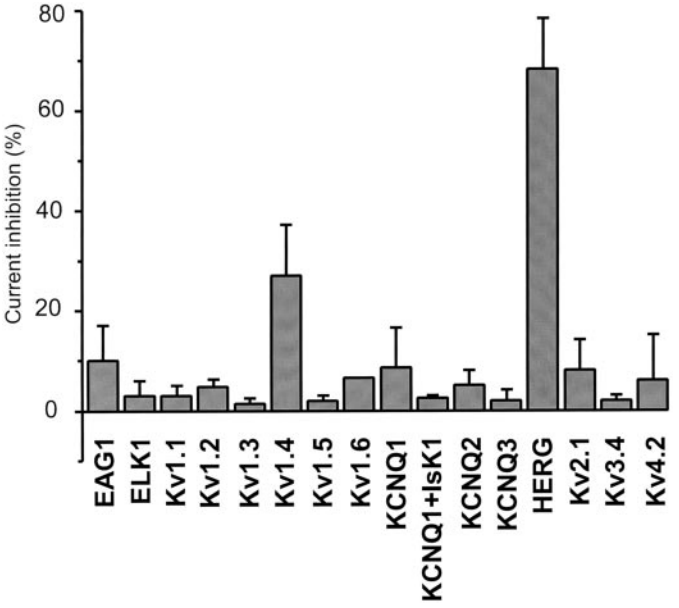

Fig. 7. Specificity of APETx1 in its action on K^+ channels. Inhibition (%) of KCNQ1–3, Kv1.1–6, Kv2.1, Kv3.4, and Kv4.2 currents by 100 nM APETx1 (n = 3 to 5 each). APETx1 (100 nM) was also tested on EAG1 and ELK1 currents (n = 5 and 6, respectively). Currents were recorded on COS-7 transfected cells and inhibitions were calculated at peak current upon depolarization to −10, 0, or +10 mV from a holding potential of = −80 mV.

APETx1 is a useful tool to separate the erg component from the M-like current ($I_{K(M,ng)}$) in NG108-15 cells. The molecular composition of this deactivating K^+ current has been attributed to the expression of ERG1/ERG2 and KCNQ2/Q3 heteromultimers (Selyanko et al., 2002). We have shown that APETx1 (100 nM) did not inhibit the KCNQ2 and KCNQ3 channels expressed in COS-transfected cells. Moreover, APETx1 (100 nM) inhibited by 50% the deactivating current in NG108-15 cells, leaving a residual outward current. KCNQ2/Q3 channels probably carry this resistant current.

APETx1 is devoid of high neurotoxicity after central injection in mice, even at high concentrations. An absence of acute neurotoxicity was also observed in previous experiments with other K^+ channel blocking toxins, such as BDS-I or spider phrixotoxins, when injected intracisternally into mice (Diochot et al., 1998, 1999). These peptides, which inhibit HERG, Kv3.4, Kv4.2, and Kv4.3 channels are not strongly neurotoxic, in contrast to Kv1 channel blockers from scorpion, bee, or snake venoms, which induce severe epileptic seizures and convulsions (Schweitz, 1984; Mourre et al., 1997). Clearly, blocking HERG channels in the brain does not kill an animal or produce drastic changes in excitability. Thus, APETx1 toxin will be useful to analyze more subtle

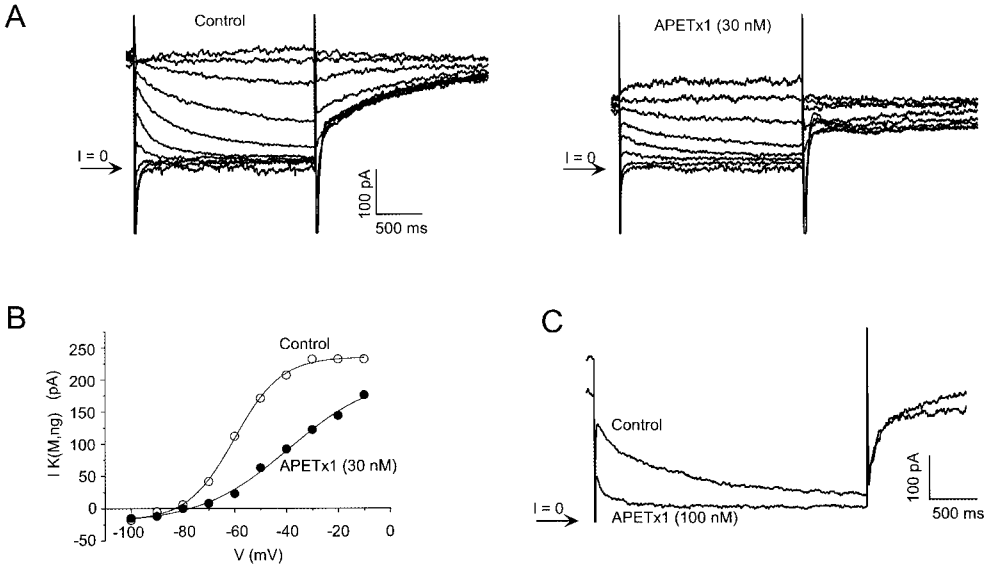

Fig. 8. Effect of APETx1 on the M-like current ($I_{K(M,ng)}$) in NG108-15 cells. A, current-voltage (IV) relations obtained during voltage steps from a holding potential of −20 mV to potentials between −10 and −100 mV. Outwardly deactivating tail currents are observed during hyperpolarizing steps and are partially inhibited during the application of 30 nM APETx1. B, the corresponding IV curve was obtained by measuring the peak of the current at the beginning of the voltage pulse before (○) and during (●) the application of 30 nM APETx1. Currents were measured with respect to zero current as indicated by the arrow on the IV traces. C, the $I_{K(M,ng)}$ current recorded at −50 mV from a holding potential of −20 mV is inhibited by 100 nM APETx1, leaving a fast deactivating component. Note that the standing outward current was also reduced significantly. The zero current is indicated by the arrow.

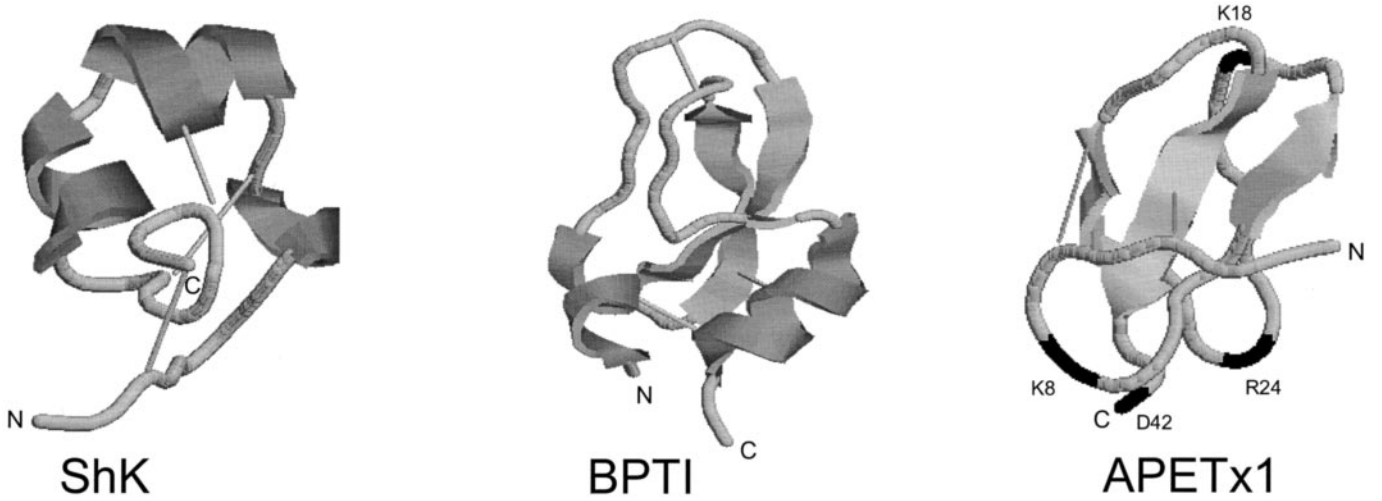

Fig. 9. Sea-anemone K^+ channel inhibitors belong to three different structural groups. Structures were prepared with the program RASMOL, using coordinates from the Protein Data Bank. C and N termini of peptides are indicated by letters. The short peptide group characterized by two short α-helices and one helical turn includes ShK, BgK, AsKS, and HmK. In the second group [basic pancreatic trypsin inhibitor (BPTI), kalicludines, and DTX_1], the structure comprises a two-stranded β-sheet and two α-helices. In the last one (APETx1 and BDS), the structure shows a triple-stranded antiparallel β-sheet without an α-helix. Location of basic residues is indicated in black.

changes of behavior produced by HERG channel blockade. The pharmacological approach is a necessary complement to the gene knockout approach that can be accompanied by compensations in gene expression.

Acknowledgments

We gratefully thank Drs. O. Pongs (eag1 and elk1) and L. Jan (KV4.2) for their generous gifts. We thank D. Moinier, S. Scarzello, M. Jodar, V. Briet, Y. Benhamou, L. Rash, and F. Lesage for technical assistance and M. Borsotto, M-D Drici, G. Romey, and P. Escoubas for helpful discussions.

References

Aneiros A, Garcia I, Martinez JR, Harvey AL, Anderson AJ, Marshall DL, Engström A, Hellman U, and Karlsson E (1993) A potassium channel toxin from the secretion of the sea anemone *Bunodosoma granulifera* Isolation, amino acid sequence and biological activity. *Biochim Biophys Acta* **1157:**86–92.

Arcangeli A, Bianchi L, Becchetti A, Faravelli L, Coronnello M, Mini E, Olivotto M, and Wanke E (1995) A novel inward-rectifying K^+ current with a cell-cycle dependence governs the resting potential of mammalian neuroblastoma cells. *J Physiol* **489:**455–471.

Awan KA and Dolly JO (1991) K^+ channel sub-types in rat brain : characteristic locations revealed using β-bungarotoxin, α and δ-dendrotoxins. *Neuroscience* **40:** 29–39.

Benzinger GR, Kyle JW, Blumenthal KM, and Hanck DA (1998) A specific interaction between the cardiac sodium channel and site-3 toxin anthopleurin B. *J Biol Chem* **273:**80–84.

Bianchi L, Wible B, Arcangeli A, Taglialatela M, Morra F, Castaldo P, Crociani O, Rosati B, Faravelli L, Olivotto M, et al. (1998) herg encodes a K^+ current highly conserved in tumors of different histogenesis: a selective advantage for cancer cells? *Cancer Res* **58:**815–822.

Bidard JN, Mourre C, Gandolfo G, Schweitz H, Widmann C, Gottesmann C, and Lazdunski M (1989) Analogies and differences in the mode of action and properties of binding sites (localization and mutual interactions) of two K^+ channel toxins, MCD peptide and dendrotoxin I. *Brain Res* **495:**45–57.

Brown DA and Adams PR (1980) Muscarinic suppression of a novel voltage-sensitive K^+ current in a vertebrate neurone. *Nature (Lond)* **283:**673–676.

Bruhn T, Schaller C, Schulze C, Sanchez-Rodriguez J, Dannmeier C, Ravens U, Heubach JF, Eckhardt K, Schmidtmayer J, Schmidt H, et al. (2001) Isolation and characterisation of five neurotoxic and cardiotoxic polypeptides from the sea anemone *Anthopleura elegantissima*. *Toxicon* **39:**693–702.

Castaneda O, Sotolongo V, Amor AM, Stocklin R, Anderson AJ, Harvey AL, Engstrom A, Wernstedt C, and Karlsson E (1995) Characterization of a potassium channel toxin from the Caribbean Sea anemone *Stichodactyla helianthus*. *Toxicon* **33:**603–613.

Chiesa N, Rosati B, Arcangeli A, Olivotto M, and Wanke E (1997) A novel role for HERG K^+ channels: spike-frequency adaptation. *J Physiol* **501:**313–318.

Chouabe C, Drici MD, Romey G, and Barhanin J (2000) Effects of calcium channel blockers on cloned cardiac K^+ channels IKr and IKs. *Therapie* **55:**195–202.

Chouabe C, Drici MD, Romey G, Barhanin J, and Lazdunski M (1998) HERG and KvLQT1/IsK, the cardiac K^+ channels involved in long QT syndromes, are targets for calcium channel blockers. *Mol Pharmacol* **54:**695–703.

Cotton J, Crest M, Bouet F, Alessandri N, Gola M, Forest E, Karlsson E, Castaneda O, Harvey AL, Vita C, et al. (1997) A potassium-channel toxin from the sea anemone *Bunodosoma granulifera*, an inhibitor for Kv1 channels. Revision of the amino acid sequence, disulfide-bridge assignment, chemical synthesis and biological activity. *Eur J Biochem* **244:**192–202.

Dauplais M, Lecoq A, Song J, Cotton J, Jamin N, Gilquin B, Roumestand C, Vita C, de Medeiros CL, Rowan EG, et al. (1997) On the convergent evolution of animal toxins. Conservation of a diad of functional residues in potassium channel-blocking toxins with unrelated structures. *J Biol Chem* **272:**4302–4309.

Diochot S, Drici MD, Moinier D, Fink M, and Lazdunski M (1999) Effects of phrixotoxins on the Kv4 family of potassium channels and implications for the role of Ito1 in cardiac electrogenesis. *Br J Pharmacol* **126:**251–263.

Diochot S, Schweitz H, Beress L, and Lazdunski M (1998) Sea anemone peptides with a specific blocking activity against the fast inactivating potassium channel Kv3.4. *J Biol Chem* **273:**6744–6749.

Drici MD, Diochot S, Terrenoire C, Romey G, and Lazdunski M (2000) The bee venom peptide tertiapin underlines the role of I_{KACh} in acetylcholine-induced atrioventricular blocks. *Br J Pharmacol* **131:**569–577.

Drici MD, Knollmann BC, Wang WX, and Woosley RL (1998) Cardiac actions of erythromycin: influence of female sex. *J Am Med Assoc* **280:**1774–1776.

Driscoll PC, Clore GM, Beress L, and Gronenborn AM (1989a) A proton nuclear magnetic resonance study of the antihypertensive and antiviral protein BDS-I from the sea anemone *Anemonia sulcata*: sequential and stereospecific resonance assignment and secondary structure. *Biochemistry* **28:**2178–2187.

Driscoll PC, Gronenborn AM, Beress L, and Clore GM (1989b) Determination of the three-dimensional solution structure of the antihypertensive and antiviral protein BDS-I from the sea anemone *Anemonia sulcata*: a study using nuclear magnetic resonance and hybrid distance geometry-dynamical simulated annealing. *Biochemistry* **28:**2188–2198.

Finlayson K, Pennington AJ, and Kelly JS (2001) [^{3}H]Dofetilide binding in SHSY5Y and HEK293 cells expressing a HERG-like K^+ channel? *Eur J Pharmacol* **412:** 203–212.

Frelin C, Vigne P, Schweitz H, and Lazdunski M (1984) The interaction of sea anemone and scorpion neurotoxins with tetrodotoxin-resistant Na^+ channels in rat myoblasts. A comparison with Na^+ channels in other excitable and non-excitable cells. *Mol Pharmacol* **26:**70–74.

Gendeh GS, Young LC, de Medeiros CL, Jeyaseelan K, Harvey AL, and Chung MC (1997) A new potassium channel toxin from the sea anemone *Heteractis magnifica*: isolation, cDNA cloning and functional expression. *Biochemistry* **36:**11461–11471.

Grissmer S, Nguyen AN, Aiyar J, Hanson DC, Mather RJ, Gutman GA, Karmilowicz MJ, Auperin DD, and Chandy KG (1994) Pharmacological characterization of five cloned voltage-gated K^+ channels, types Kv1.1, 1.2, 1.3, 1.5, and 3.1, stably expressed in mammalian cell lines. *Mol Pharmacol* **45:**1227–1234.

Gurrola GB, Rosati B, Rocchetti M, Pimienta G, Zaza A, Arcangeli A, Olivotto M, Possani LD, and Wanke E (1999) A toxin to nervous, cardiac and endocrine ERG K^+ channels isolated from *Centruroides noxius* scorpion venom. *FASEB J* **13:**953–962.

Hugues M, Romey G, Duval D, Vincent JP, and Lazdunski M (1982) Apamin as a selective blocker of the calcium-dependent potassium channel in neuroblastoma cells: voltage-clamp and biochemical characterization of the toxin receptor. *Proc Natl Acad Sci USA* **79:**1308–1312.

Johnson WC Jr (1985) Circular dichroism and its empirical application to biopolymers. *Methods Biochem Anal* **31:**61–163.

Korolkova YV, Kozlov SA, Lipkin AV, Pluzhnikov KA, Hadley JK, Filippov AK, Brown DA, Angelo K, Strobaek D, Jespersen T, et al. (2001) An ERG channel inhibitor from the scorpion *Buthus eupeus*. *J Biol Chem* **276:**9868–9876.

Lancelin JM, Foray MF, Poncin M, Hollecker M, and Marion D (1994) Proteinase inhibitor homologues as potassium channel blockers. *Nat Struct Biol* **1:**246–250.
Loret EP, del Valle RM, Mansuelle P, Sampieri F, and Rochat H (1994) Positively charged amino acid residues located similarly in sea anemone and scorpion toxins. *J Biol Chem* **269:**16785–16788.
Meves H, Schwarz JR, and Wulfsen I (1999) Separation of M-like current and ERG current in NG108-15 cells. *Br J Pharmacol* **127:**1213–1223.
Moczydlowski E, Lucchesi K, and Ravidran A (1988) An emerging pharmacology of peptide toxins targeted against potassium channels. *J Membr Biol* **105:**95–111.
Mourre C, Lazdunski M, and Jarrard LE (1997) Behaviors and neurodegeneration induced by two blockers of K^+ channels, the mast cell degranulating peptide and dendrotoxin I. *Brain Res* **762:**223–227.
Norton RS (1991) Structure and structure-function relationships of sea anemone proteins that interact with the sodium channel. *Toxicon* **29:**1051–1084.
Pardo-Lopez L, Zhang M, Liu J, Jiang M, Possani LD, and Tseng GN (2002) Mapping the binding site of a human ether-a-go-go-related gene-specific peptide toxin (ErgTx) to the channel's outer vestibule. *J Biol Chem* **277:**16403–16411.
Rauer H, Pennington M, Cahalan M, and Chandy KG (1999) Structural conservation of the pores of calcium-activated and voltage-gated potassium channels determined by a sea anemone toxin. *J Biol Chem* **274:**21885–21892.
Renaud JF, Fosset M, Schweitz H, and Lazdunski M (1986) The interaction of polypeptide neurotoxins with tetrodotoxin-resistant Na^+ channels in mammalian cardiac cells. Correlation with inotropic and arrhythmic effects. *Eur J Pharmacol* **120:**161–170.
Robbins J, Trouslard J, Marsh SJ, and Brown DA (1992) Kinetic and pharmacological properties of the M-current in rodent neuroblastoma x glioma hybrid cells. *J Physiol* **451:**159–185.
Romey G, Abita J-P, Schweitz H, Wunderer G, and Lazdunski M (1976) Sea anemone toxins: a tool to study the mechanism of nerve conduction and excitation-secretion coupling. *Proc Natl Acad Sci USA* **73:**4055–4059.
Sanguinetti MC, Curran ME, Spector PS, and Keating MT (1996) Spectrum of HERG K^+-channel dysfunction in an inherited cardiac arrhythmia. *Proc Natl Acad Sci USA* **93:**2208–2212.
Sanguinetti MC, Jiang C, Curran ME, and Keating MT (1995) A mechanistic link between an inherited and an acquired cardiac arrhythmia: HERG encodes the IKr potassium channel. *Cell* **81:**299–307.
Sanguinetti MC and Jurkiewicz NK (1990) Two components of cardiac delayed rectifier K^+ current. Differential sensitivity to block by class III antiarrhythmic agents. *J Gen Physiol* **96:**195–215.
Schweitz H (1984) Lethal potency in mice of toxins from scorpion, sea anemone, snake and bee venoms following intraperitoneal and intracisternal injection. *Toxicon* **22:**308–311.
Schweitz H, Bidard JN, Maes P, and Lazdunski M (1989) Charybdotoxin is a new member of the K^+ channel toxin family that includes dendrotoxin I and mast cell degranulating peptide. *Biochemistry* **28:**9708–9714.
Schweitz H, Bruhn T, Guillemare E, Moinier D, Lancelin J-M, Béress L, and Lazdunski M (1995) Kalicludines and Kaliseptine: two different classes of sea anemones toxins for voltage-sensitive K^+ channels. *J Biol Chem* **270:**25121–25126.
Selyanko AA, Delmas P, Hadley JK, Tatulian L, Wood IC, Mistry M, London B, and Brown DA (2002) Dominant-negative subunits reveal potassium channel families that contribute to M-like potassium currents. *J Neurosci* **22:**RC212.
Snyders DJ and Chaudhary A (1996) High affinity open channel block by dofetilide of HERG expressed in a human cell line. *Mol Pharmacol* **49:**949–955.
Spector PS, Curran ME, Keating MT, and Sanguinetti MC (1996) Class III antiarrhythmic drugs block HERG, a human cardiac delayed rectifier K^+ channel. Open-channel block by methanesulfonanilides. *Circ Res* **78:**499–503.
Suessbrich H, Schonherr R, Heinemann SH, Attali B, Lang F, and Busch AE (1997) The inhibitory effect of the antipsychotic drug haloperidol on HERG potassium channels expressed in *Xenopus* oocytes. *Br J Pharmacol* **120:**968–974.
Swartz KJ and MacKinnon R (1995) An inhibitor of the Kv2.1 potassium channel isolated from the venom of a Chilean tarantula. *Neuron* **15:**941–949.
Taglialatela M, Pannaccione A, Castaldo P, Giorgio G, Zhou Z, January CT, Genovese A, Marone G, and Annunziato L (1998) Molecular basis for the lack of HERG K^+ channel block-related cardiotoxicity by the H1 receptor blocker cetirizine compared with other second-generation antihistamines. *Mol Pharmacol* **54:**113–121.
Trudeau MC, Warmke JW, Ganetzky B, and Robertson GA (1995) HERG, a human inward rectifier in the voltage-gated potassium channel family. *Science (Wash DC)* **269:**92–95.
Tytgat J, Chandy KG, Garcia ML, Gutman GA, Martin-Eauclaire MF, van der Walt JJ, and Possani LD (1999) A unified nomenclature for short-chain peptides isolated from scorpion venoms: alpha-KTx molecular subfamilies. *Trends Pharmacol Sci* **20:**444–447.

Address correspondence to: Prof. Michel Lazdunski, Institut de Pharmacologie moléculaire et Cellulaire, CNRS- UMR6097, 660 Route des Lucioles, Sophia-Antipolis, 06560 Valbonne, France. E-mail: ipmc@ipmc.cnrs.fr